Geomechanics and Engineering, *Vol. 24, No. 5 (2021) 491-503*
DOI: https://doi.org/10.12989/gae.2021.24.5.491

Limit analysis of seismic collapse for shallow tunnel in inhomogeneous ground

Zihong Guo*[1,2], Xinrong Liu[3a] and Zhanyuan Zhu[1,2b]

[1]*College of Civil Engineering, Sichuan Agricultural University, Dujiangyan, Sichuan, 611830, China*
[2]*Sichuan Higher Institution Engineering Research Center of Rural Construction Disaster Prevention and Reduction, Dujiangyan, 611830, China*
[3]*School of Civil Engineering, Chongqing University, Chongqing 400045, China*

(Received September 4, 2017, Revised March 7, 2021, Accepted March 9, 2021)

Abstract. Shallow tunnels are vulnerable to earthquakes, and shallow ground is usually inhomogeneous. Based on the limit equilibrium method and variational principle, a solution for the seismic collapse mechanism of shallow tunnel in inhomogeneous ground is presented. And the finite difference method is employed to compare with the analytical solution. It shows that the analytical results are conservative when the horizontal and vertical stresses equal the static earth pressure and zero at vault section, respectively. The safety factor of shallow tunnel changes greatly during an earthquake. Hence, the cyclic loading characteristics should be considered to evaluate tunnel stability. And the curve sliding surface agrees with the numerical simulation and previous studies. To save time and ensure accuracy, the curve sliding surface with 2 undetermined constants is a good choice to analyze shallow tunnel stability. Parameter analysis demonstrates that the horizontal semiaxis, acceleration, ground cohesion and homogeneity affect tunnel stability greatly, and the horizontal semiaxis, vertical semiaxis, tunnel depth and ground homogeneity have obvious influence on tunnel sliding surface. It concludes that the most applicable approaches to enhance tunnel stability are reducing the horizontal semiaxis, strengthening cohesion and setting the tunnel into good ground.

Keywords: shallow tunnel; seismic collapse; inhomogeneous ground; limit analysis; variational principle

1. Introduction

Tunnel construction is a common way to utilize underground space and plays a highly important role in infrastructure building. It was generally believed that tunnels are capable of supporting earthquake load, but this belief changed after the Chi-Chi earthquake (Wang *et al.*2001) and the Wenchuan earthquake (Wang *et al.*2013). An investigation of 52 tunnels after the Wenchuan earthquake, showed that shallow tunnels in soft ground are susceptible to the earthquake damage (Shen *et al.*2014). However, shallow tunnels are widely used to make traveling convenient and to reduce engineering costs (Yang *et al.*2011). Therefore, the seismic analysis of shallow tunnels has attracted increasing attention.

Numerical simulation is often applied to analyze seismic characteristics of shallow tunnels, such as the effect of liquefaction and different clay deposits (Azadi and Hosseini 2010, Amorosi *et al.* 2009, Gomes *et al.* 2015). Furthermore, model tests are a good way to analyze and validate shallow tunnel's dynamic response and collapse mechanism (Tao *et al.* 2015, Lei *et al.*2015). To save time and cost, researchers devote themselves to studying a reliable and convenient method for analyzing shallow tunnel stability. The limit equilibrium method is widely used to study shallow tunnel stability and supporting pressure (Fraldi *et al.* 2012, Yang *et al.* 2015) because of its easy execution and applicability.

Terzaghi failure mode was combined with the limit method to evaluate the supporting pressure for shallow tunnels. Based on the failure mode, a method to calculate the surrounding rock pressure on a shallow tunnel was established using linear and nonlinear failure criteria (Lei *et al.*2014), and the linear sliding surfaces were considered in the analysis. Upper and lower bound stability solutions were derived for tunnel collapse with the broken line sliding surface (Davis *et al.* 1980) and this sliding surface was applied to analyze the safety factor for a shallow tunnel in saturated soil with the strength reduction technique (Huang *et al.*2012). The mechanisms of shallow tunnel for curve sliding surface collapse based on nonlinear Hoek-Brown failure criterion were presented (Yang *et al.* 2011, Fraldi *et al.*2009) and the occurrence of progressive failure in tunnel roofs was analyzed (Fraldi *et al.* 2012). Numerical simulations and model tests were applied to analyze shallow tunnel stability and the results show that the sliding surface resembles a curve (Lei *et al.* 2015, Sterpi *et al.* 2004, Yamamoto *et al.* 2011). However, it is still difficult to describe shallow tunnel's sliding surface accurately.

Tunnel section changes widely to meet some special requirement. The influence of tunnel geometry on shallow tunnel stability was obvious (Davis *et al.* 1980, Fraldi *et al.* 2009, Atkinson *et al.* 1977), so it is important to take tunnel section into account to evaluate shallow tunnel stability. The ground is generally defined as homogenous material to

*Corresponding author, Professor
E-mail: guozihonghyx@126.com
[a]Professor
E-mail: liuxrong@126.com
[b]Professor
E-mail: zhuzyuan910@163.com

ISSN: 2005-307X (Print), 2092-6219 (Online)

simplify the calculation. However, this assumption occasionally has obvious influence on the accuracy of analysis. Geotechnical variability is a complex attribute that is the result of many disparate sources of uncertainty (Phoon *et al.* 1999). The inherent spatial variability of the soil shear strength can drastically modify the basic form of the failure mechanism (Popescu *et al.* 2005). The inhomogeneity of the ground was taken into account to study ground surface vibration and to propose a stochastic slope stability analysis method (Jones *et al.* 2012, Wang *et al.* 2016). Defining inhomogeneous soil's characteristics is an issue worth greater study.

The peak acceleration was regarded as a constant and applied to study tunnel stability in the pseudostatic method (Sahoo *et al.* 2014). There are many parameters which influence the acceleration distribution around tunnel where acceleration typically changes (Amorosi *et al.* 2009, Argyroudis *et al.* 2012). In a field, understanding how to define the variation of acceleration around the tunnel is an important issue to analyze tunnel seismic characteristics. A simple relationship between acceleration and soil depth was established to analyze the seismic design of the retaining wall (Munwar *et al.* 2010, Kolathayar *et al.* 2009, Ghosh *et al.* 2010) and it helps the seismic analysis of shallow tunnel.

Shallow tunnels are susceptible to earthquake damage and the ground is often inhomogeneous at the shallow layers. However, the distribution of sliding surface for shallow tunnel cannot be accurately acquired and the inhomogeneous ground is often regarded as homogeneous material to simplify analysis. The purpose of this paper aims to present a solution to analyze the seismic collapse mechanism of shallow tunnel in inhomogeneous ground. The finite difference method and previous studies were compared with the analytical method. In addition, many parameters have been analyzed in detail to propose advice on enhancing the seismic stability of the shallow tunnel in inhomogeneous ground.

2. Shallow tunnel model

A shallow tunnel in inhomogeneous ground during an earthquake is shown in Fig. 1, where a is the horizontal semiaxis, b is the vertical semiaxis, q is the supporting pressure, q' is the surface load, h_1 is the tunnel depth, H is the vertical distance from the ground surface to the tunnel bottom, γ is unit weight of soil, c is the soil cohesion, f is the soil friction coefficient, F_h and F_v are the horizontal and vertical forces at vault section AB, which equal the integral of the normal and shear stress at this section. The area $A_{CDD'C'}$ is often regarded as the roof collapse district. The coordinates of start point C and end point D at a sliding surface are (x_0, y_0) and (x_1, y_1).

The earthquake acceleration coefficient is regarded as a constant to analyze tunnel stability (Sahoo *et al.* 2014). Excavating a tunnel will change the seismic characteristics of the ground and the horizontal acceleration increases near the tunnel (Pitilakis *et al.* 2014). There are many factors with influence on the seismic characteristics and the acceleration may change greatly from the ground surface to the tunnel bottom. With the assumption that the

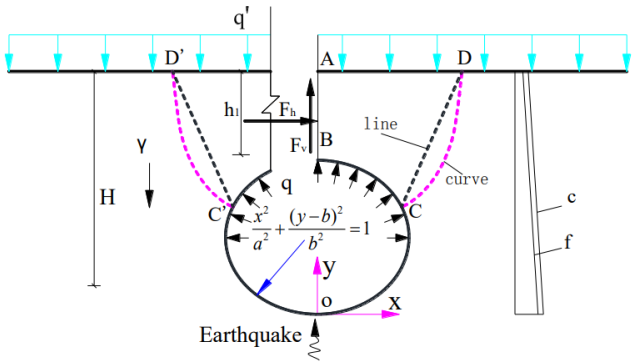

Fig. 1 A shallow tunnel model

accelerations have a relationship with depth and time, the seismic stability of the retaining wall is analyzed (Munwar *et al.* 2010, Kolathayar *et al.* 2009, Ghosh *et al.* 2010). The equations have three obvious characteristics. First, the maximum acceleration decreases with the ground depth, and it is consistent with tunnel seismic analysis (Amorosi *et al.* 2009, Bilotta *et al.* 2007). Second, the direction of acceleration is uniform at the same time in a field, and it is applied to the pseudostatic analysis of tunnel stability (Sahoo *et al.* 2014, Saada *et al.*2013). Third, the phase of acceleration can vary with time and it is useful to analyze tunnel stability with time. The acceleration coefficients are applied to shallow tunnel's seismic analysis.

$$k_h = k_{h0}\left[1+(f_a-1)\,y/H\right]\sin\omega(t-y/V_s) \tag{1}$$

$$k_v = k_{v0}\left[1+(f_a-1)\,y/H\right]\sin\omega(t-y/V_p) \tag{2}$$

where k_h and k_v are the horizontal and vertical seismic acceleration coefficients at depth $H-y$ and time t, k_{h0} is the amplitude of the horizontal acceleration coefficients and k_{v0} is the amplitude of the vertical acceleration coefficients at tunnel bottom, f_a is amplification factor, equal to the rate of the acceleration at ground surface to the acceleration at the tunnel bottom, ω is angular frequency, V_s and V_p are shear wave velocity and primary wave velocity.

For the most part the soil mechanic parameters at the surface are the lowest value and these increase with the depth. The stability of unsupported twin tunnels is analyzed on the basis that soil cohesion increases almost linearly with depth (Sahoo *et al.*2013). On the assumption that soil gravity γ, cohesion c and friction coefficient f have a linear relationship with soil depth, it can be written as

$$\gamma = \gamma_0 - \gamma_1\, y/H \tag{3}$$

$$c = c_0 - c_1\, y/H \tag{4}$$

$$f = \tan\phi_0 - \tan\phi_1\, y/H = f_0 - f_1\, y/H \tag{5}$$

where γ_0, c_0 and f_0 is soil unit weight, cohesion and friction coefficient at tunnel bottom, respectively; γ_1, c_1 and f_1 is the varying value of soil unit weight, cohesion and friction coefficient from the surface to the tunnel bottom,

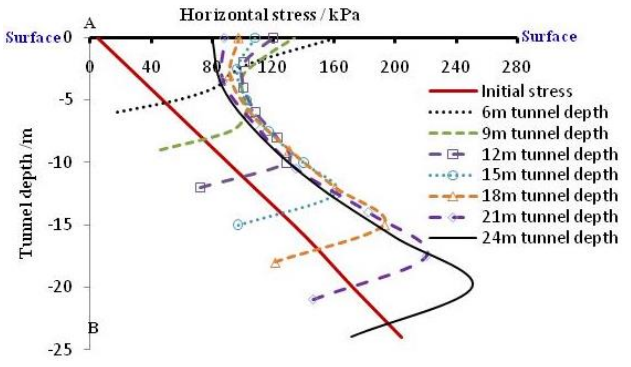

Fig. 2 Variation of horizontal stress

respectively.

The stress distribution in the ground is the earth stress at rest before the tunnel excavation. There are two methods to calculate the coefficient of earth stress at rest. First, the stress coefficient is defined as $k_0=\mu(1-\mu)$ for plane strain according to the elastic theory, where μ is Poisson ratio. Second, the stress coefficient equals $1-\sin\varphi$ according to the Jaky equation (Jaky *et al.*1944), where φ is the inner friction angle. The stress around tunnel will change widely after the tunnel is excavated. If k_h equals zero, F_v is zero because of the symmetry of the load and structure. On the contrary, F_v does not equal zero when k_h isn't zero.

The finite difference method was applied to analyze the stress distribution in the shallow tunnel. The variation of horizontal stress is shown in Fig. 2. The initial stress increases with the tunnel depth. After excavation, the horizontal stress shows an increase at the most parts of vault section AB, and the increasing value is most obvious at the surface. The horizontal stress decreases only in a little area close to the tunnel. In a word, the excavation of shallow tunnel leads to the increase of the mean horizontal stress at section AB. Therefore, the stress at section AB is more than the static earth pressure.

3. Seismic analysis for shallow tunnel

3.1 Collapse mechanism with linear sliding surface

Terzaghi theory was used to calculate the surrounding rock pressure on the base of the limit equilibrium method and linear sliding surface. According to Terzaghi failure mode, a method was presented to analyze the surrounding rock pressure of the shallow tunnel with linear and nonlinear failure criteria (Lei *et al.* 2014). On the hypothesis that sliding surface is linear, shallow tunnel's safety factor k_{sl} can be defined as the ratio of the shear strength to the shear force along a sliding surface.

$$k_{sl}=\frac{cl+\overline{f}\left[W(1+k_v)\cos\alpha+F_h\sin\alpha-F_v\cos\alpha-qx_0\cos\alpha+q(2b-y_0)\sin\alpha-Q\sin\alpha+q'x_1\cos\right.}{W(1+k_v)\sin\alpha+Q\cos\alpha-F_h\cos\alpha-F_v\sin\alpha-q(2b-y_0)\cos\alpha-qx_0\sin\alpha+q'x_1\sin\alpha} \quad (6)$$

$$cl=\int_{y_0}^{H}(c_0-c_1\,y/H)\sqrt{1+k^{-2}}\,dy \quad (7)$$

$$\overline{f}=\tan\phi_0-\tan\phi_1\left(y_0+H\right)/2H \quad (8)$$

$$\cos\alpha=1/\sqrt{1+k^2} \quad (9)$$

$$\cos\alpha=1/\sqrt{1+k^2} \quad (10)$$

$$\begin{aligned}W(1+k_v)&=\int_{y_0}^{2b}\left[x-a/b\sqrt{b^2-(y-b)^2}\right]\gamma(y)(1+k_v)dy+\int_{2b}^{H}x\gamma(y)(1+k_v)dy\\&=\int_{y_0}^{2b}\left[(y-y_0)/k+x_0-a/b\sqrt{b^2-(y-b)^2}\right]\gamma(y)(1+k_v)dy+\int_{2b}^{H}\left[(y-y_0)/k+x_0\right]\gamma(y)(1+k_v)dy\end{aligned} \quad (11)$$

$$\begin{aligned}Q&=\int_{y_0}^{2b}\left[x-a/b\sqrt{b^2-(y-b)^2}\right]\gamma(y)k_h dy+\int_{2b}^{H}x\gamma(y)k_h dy\\&=\int_{y_0}^{2b}\left[(y-y_0)/k+x_0-a/b\sqrt{b^2-(y-b)^2}\right]\gamma(y)k_h dy+\int_{2b}^{H}\left[(y-y_0)/k+x_0\right]\gamma(y)k_h dy\end{aligned} \quad (12)$$

$$x=\left(y-y_0\right)/k+x_0 \quad (13)$$

$$y_0=b+\sqrt{b^2-(b/a\,x_0)^2} \quad (14)$$

where k is the slope for the sliding surface, W is the gravity of soil and Q is the horizontal body force induced by earthquake in the area A_{ABCD}. To solve the extremum problem, K_{sl} must satisfy the following requirements and it can be solved with the numerical method.

$$\frac{\partial k_{sl}}{\partial x_0}=0,\ \frac{\partial k_{sl}}{\partial k}=0 \quad (15)$$

3.2 Collapse mechanism with curve sliding surface

The model test shows that the sliding surface of shallow tunnel is not linear (Lei *et al.*2015). The broken line sliding surface was applied to analyze shallow tunnel stability and collapse mechanism (Davis *et al.* 1980, Huang *et al.* 2012, Yamamoto *et al.* 2011). In addition, the limit analysis of collapse mechanisms for a circular tunnel was carried out to analyze shallow tunnel stability and their results showed that the sliding surface is a curve (Fraldi *et al.* 2009, Huang *et al.*2011). The shallow tunnel's sliding surface distribution is still an unsolved issue. A definite sliding surface may affect the analytical results of the shallow tunnel. Therefore, it is a good choice to define a function which is suitable to any curve sliding surfaces. A small horizontal slice is taken from Fig. 1 and it is shown in Fig. 3.

The forces need balancing in the x'-axis direction, and the equation can be written as

$$\sum F_{x'}=0,\quad S_i=Q_i\cos\alpha_i-\Delta E_i\sin\alpha+W_i(1+k_v)\sin\alpha_i-F_{hi}\cos\alpha_i-F_{vi}\sin\alpha_i=(c_i l_i+N_i f_i)/k_{sc} \quad (16)$$

where S_i and N_i is the shear strength and the normal force on the small surface; α_i is the angle between x'-axis and x-axis; ΔE_i is the resultant of the forces at the slice's surface and bottom; F_{hi} and F_{vi} are the vertical and horizontal forces at section AB; W_i is the gravity of the slice; Q_i is the horizontal body force of the slice induced by earthquake. The equation (11) can be rewritten as

$$\Delta E_i = W_i(1+k_v) + Q_i\cot\alpha_i - F_{hi}\cot\alpha_i - F_{vi} - (c_i l_i + N_i f_i)\csc\alpha_i / k_{sc} \quad (17)$$

The resultant of all ΔE_i should equal the sum of the surface load and the supporting force in y-direction.

$$\begin{aligned}&\sum_1^n W_i(1+k_v) + \sum_1^n Q_i\cot\alpha_i - \sum_1^n F_{hi}\cot\alpha_i - \sum_1^n F_{vi} - \sum_1^n (c_i l_i + N_i f_i)\csc\alpha_i / k_{sc} \\ &= qr\sin\beta - q'x_1 = qx_0 - q'x_1\end{aligned} \quad (18)$$

Next, the shallow tunnel's safety factor can be derived as

$$k_{sc} = \frac{\sum_1^n \csc\alpha_i (c_i l_i + N_i f_i)}{\sum_1^n W_i(1+k_v) + \sum_1^n Q_i\cot\alpha_i - \sum_1^n F_{hi}\cot\alpha_i - F_v - qx_0 + q'x_1} \quad (19)$$

The forces should be balanced at y'-axis direction, and the equation can be written as

$$\begin{aligned}&\sum y' = 0, \quad N_i = W_i(1+k_v)\cos\alpha_i - E_i\cos\alpha_i - Q_i\sin\alpha_i + F_{hi}\sin\alpha_i - F_{vi}\cos\alpha_i \\ &\csc\alpha_i N_i = W_i(1+k_v)\cot\alpha_i - E_i\cot\alpha_i - Q_i + F_{hi} - F_{vi}\cot\alpha_i\end{aligned} \quad (20)$$

The resultant of all $\csc\alpha_i N_i$ can be derived as

$$\sum_1^n \csc\alpha N_i = \sum_1^n W_i(1+k_v)\cot\alpha_i - \sum_1^n Q_i + F_h - \sum_1^n \Delta E_i\cot\alpha_i - \sum_1^n F_{vi}\cot\alpha_i \quad (21)$$

The sum of all ΔE_i equals $qx_0 - q'x_1$. q' and q only exist at the ground surface and the tunnel boundary, so the sum of all $\Delta E_i\cot\alpha_i$ is defined as $(qx_0 - q'x_1)\cot\alpha$ to simplify the calculation, where α is the angle for the slope of l_{CD}. Then, Eq. (20) is rewritten as

$$\begin{aligned}&\sum_1^n \csc\alpha N_i = \sum_1^n W_i(1+k_v)\cot\alpha - \sum_1^n Q_i + F_h - \sum_1^n F_{vi}\cot\alpha_i + (q_1x_1 - qx_0)\cot\alpha \\ &\cot\alpha = (x_1 - x_0)\Big/\left(H - h - \sqrt{r^2 - x_0^2}\right)\end{aligned} \quad (22)$$

where F_{hi} and F_{vi} are not continuous along the sliding surface. To establish a continuous function for the sliding surface, the following equations are defined.

$$\sum_1^n F_{vi}\cot\alpha_i = F_v\cot\alpha, \ \sum_1^n F_{hi}\cot\alpha_i = F_h\cot\alpha \quad (23)$$

and then Eq. (19) is rewritten as

$$k_{sc} = \frac{\sum_1^n c_i l_i\csc\alpha_i + \left[\sum_1^n f_i W_i(1+k_v)\cot\alpha_i - \sum_1^n f_i Q_i + \overline{f}\left(F_h - F_v\cot\alpha + q_1x_1\cot\alpha - qx_0\cot\alpha\right)\right]}{\sum_1^n W_i(1+k_v) + \sum_1^n Q_i\cot\alpha_i - F_h\cot\alpha - F_v - qx_0 + q'x_1} \quad (24)$$

When α_i is more than 90° the second part of the numerator in Eq. (24) may be negative. However, it is unreasonable because the friction force direction is always contrary to the movement direction. Therefore, the second part of the numerator should be kept positive.

If point C is regarded as the origin point each part of Eq. (24) can be written as

$$\sum_1^n c_i l_i\csc\alpha = \int_0^{H-y_0} c\left(1 + x'^2\right)dy \quad (25)$$

$$\begin{aligned}&\sum_1^n f_i W_i(1+k_v)\cot\alpha_i = \int_0^{2b-y_0} f_i[x + x_0 - l_x]\gamma_y(1+k_v)x'dy + \int_{2b-y_0}^{H-y_0} f_i(x+x_0)\gamma_y(1+k_v)x'dy \\ &l_x = a/b\sqrt{b^2 - (y-b+y_0)^2}\end{aligned} \quad (26)$$

$$\sum_1^n f_i Q_i = \int_0^{2b-y_0} f_y(x + x_0 - l_x)\gamma_y k_h dy + \int_{2b-y_0}^{H-y_0} f_y(x+x_0)\gamma_y k_h dy \quad (27)$$

$$\sum_1^n W_i(1+k_v) = \int_0^{2b-y_0}(x + x_0 - l_x)\gamma_y(1+k_v)dy + \int_{2b-y_0}^{H-y_0}(x+x_0)\gamma_y(1+k_v)dy \quad (28)$$

$$\sum_1^n Q_i\cot\alpha_i = \int_0^{2b-y_0}(x + x_0 - l_x)\gamma_y k_h x'dy + \int_{2b-y_0}^{H-y_0}(x+x_0)\gamma_y k_h x'dy \quad (29)$$

where the horizontal and vertical seismic acceleration coefficients, density, cohesion and friction coefficients should be rewritten as

$$k_h = k_{h0}\left[1 + (f_a - 1)(y + y_0)/H\right]\sin\omega\left[t - (y + y_0)/V_s\right] \quad (30)$$

$$k_v = k_{v0}\left[1 + (f_a - 1)(y + y_0)/H\right]\sin\omega\left[t - (y + y_0)/V_p\right] \quad (31)$$

$$\gamma = \gamma_0 - \gamma_1(y + y_0)/H \quad (32)$$

$$c = c_0 - c_1(y + y_0)/H \quad (33)$$

$$f = \tan\phi = \tan\phi_0 - \tan\phi_1(y + y_0)/H \quad (34)$$

The shallow tunnel safety factor $k_{sc}(x,y)$ is a functional. The following boundary conditions should be met.

$$x_{y=0} = 0, \qquad x_{y=H-y_0} = x_1 - x_0 \quad (35)$$

To change the inhomogeneous boundary conditions into the homogeneous boundary conditions, function z is defined as

$$z = y - x(H - y_0)/(x_1 - x_0) \quad (36)$$

$$x = (x_1 - x_0)(y - z)/(H - y_0) \quad (37)$$

$$z_{y=0} = 0, \qquad z_{y=H-y_0} = 0 \quad (38)$$

Eqs. (24) and (36) satisfy the boundary conditions Eq. (35). According to Ritz method the basis function $z_n(y)$ can be defined as

$$z_n(y) = \sum_{k=1}^n a_n y^n (y - H + y_0) \quad (39)$$

where a_n is an undetermined constant. To solve the minimum for k_{sc}, the following conditions should be satisfied.

$$\frac{\partial k_{sc}}{\partial x_0} = 0, \ \frac{\partial k_{sc}}{\partial x_1} = 0 \quad (40)$$

$$\frac{\partial k_{sc}}{\partial a_1} = 0, \frac{\partial k_{sc}}{\partial a_2} = 0, \ldots, \frac{\partial k_{sc}}{\partial a_n} = 0 \quad (41)$$

The sliding surface and safety factor for the shallow tunnel can be acquired according to Eqs. (40) and (41). The number n influences the accuracy and the time of calculation. There are many factors influencing the sliding surface and the safety factor. These factors will be discussed with numerical method in the following.

4. Discussion

4.1 Choice for the forces at vault

After the construction of a shallow tunnel in the ground, the stress concentration occurs around the tunnel. The earthquake creates stress change in the ground as well. To properly select stress at section AB, the influences of forces F_h and F_v on shallow tunnel's safety factor and sliding surface are analyzed on the assumption that stress coefficient equals $k0=\mu(1-\mu)$ for plane strain.

A shallow tunnel is built in the ground, where a=6 m, b=5 m, q'=20 kPa, q=20 kPa, h_1=6 m, f_a=1.3,μ=0.3, $k_v=k_h$=0.3, f_0=0.7, f_1=0.3, c_0=200 kPa, c_1=90 kPa, γ_0=20 kN/m^3 and γ_1=3 kN/m^3. Then, the integral of static earth pressure F_0 is 186 kN. Not taking the vertical pressure into account, the linear and curve sliding surface with 2 undetermined constants are applied to analyze the horizontal force's influence on shallow tunnel collapse, as shown in Table 1. When F_h increases from F_0 to 2.2F_0, the results with curve sliding surface show that K_{sc}, x_0, x_1, a_1 and a_2 change from 0.947, 5.839 m, 8.938 m, 1.474×10^{-1} and -4.465×10^{-3} to 1.049, 5.916 m, 9.148 m, 1.569×10^{-1} and -5.518×10^{-3}, respectively, and the results with linear sliding surface show that K_{sl}, x_0, and x_1 change from 1.031, 5.695 m and 8.807 m to 1.152, 5.803 m and 8.967 m, respectively. It is clear that the greater the horizontal force is, the greater the safety factor becomes. The increase of horizontal force leads to the increase of x_0 and x_1. And the safety factors on curve sliding surfaces are less than the results on linear sliding surfaces.

When all parameters are fixed with $F_h=F_0$, the vertical force influence on shallow tunnel collapse is shown in Table 2. On the linear sliding surface k_{sl}, x_0 and x_1 increase from 1.031, 5.695 m and 8.807 m to 1.094, 5.796 m and 9.532 m, respectively, while the vertical force F_v increases from 0 to 0.6F_h, meanwhile, K_{sc}, x_0, x_1, a_1 and a_2 change from 0.947, 5.839 m, 8.938 m, $1.474\times10^{-1}$and -4.465×10^{-3} to 0.998, 5.909 m, 9.557 m, $1.283\times10^{-1}$and -2.773×10^{-3} on the curve sliding surface, respectively. It shows that the vertical force F_v leads to the increase of the safety factor and collapse area. The safety factor with linear sliding surface is greater than with curve sliding surface.

Table 1 Horizontal force's influence on shallow tunnel collapse

F_h/F_0		1	1.2	1.4	1.6	1.8	2	2.2
Curve sliding surface	k_{sc}	0.947	0.964	0.981	0.998	1.015	1.032	1.049
	x_0 (m)	5.839	5.854	5.872	5.882	5.895	5.905	5.916
	x_1 (m)	8.938	8.977	9.028	9.052	9.094	9.117	9.148
	$a_1(10^{-1})$	1.474	1.491	1.499	1.522	1.527	1.551	1.569
	$a_2(10^{-3})$	-4.465	-4.651	-4.755	-4.998	-5.064	-5.315	-5.518
Linear sliding surface	k_{sl}	1.031	1.051	1.071	1.091	1.111	1.132	1.152
	x_0 (m)	5.695	5.716	5.736	5.755	5.772	5.788	5.803
	x_1 (m)	8.807	8.843	8.875	8.904	8.929	8.950	8.967

Table 2 Vertical force influence on shallow tunnel collapse

F_v/F_h		0	0.1	0.2	0.3	0.4	0.5	0.6
Curve sliding surface	k_{sc}	0.947	0.956	0.964	0.972	0.981	0.989	0.998
	x_0 (m)	5.839	5.850	5.864	5.876	5.886	5.898	5.909
	x_1 (m)	8.938	9.029	9.139	9.244	9.343	9.450	9.557
	$a_1(10^{-1})$	1.474	1.450	1.410	1.375	1.345	1.314	1.283
	$a_2(10^{-3})$	-4.465	-4.256	-3.882	-3.572	-3.305	-3.039	-2.773
Linear sliding surface	k_{sl}	1.031	1.042	1.052	1.062	1.073	1.083	1.094
	x_0 (m)	5.695	5.713	5.731	5.748	5.765	5.781	5.796
	x_1 (m)	8.807	8.926	9.045	9.166	9.287	9.409	9.532

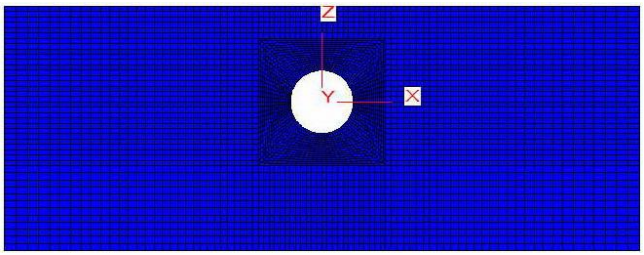

Fig. 4 Numerical model of shallow tunnel

Both horizontal and vertical forces at section AB influence shallow tunnel stability. The finite difference method (FLAC^{3D}) is employed to analyze the safety factor of shallow tunnel and to compare with the analytical method. The numerical model of shallow tunnel is shown in Fig. 4. The ground is taken as Mohr-Columb material, the bottom boundary is fixed in Z-direction displacement, the left and right boundaries are fixed in X-direction displacement, the front and behind boundaries are fixed in Y-direction displacement, and the surface load and supporting pressure can be applied on the ground surface and tunnel surface, respectively. The pseudo-static seismic acceleration is employed to analyze shallow tunnel (Sahoo *et al.*2014) and it is compatible with Eq. (1) and (2).

Two examples of shallow tunnel are taken into account. Their same parameters are a=6 m, b=6 m, h_1=6 m, q'=40 kPa, q=20 kPa, f_a=1.3, $k_h=k_v$=0.3 and ν=0.3. Their ground parameters are different. One tunnel is located in the homogeneous ground where friction coefficient is 0.47, cohesion is 180 kPa and unit weight is 20 kN/m^3. Another tunnel is located in the inhomogeneous ground where f_0=0.70, f_1=0.30, c_0=200 kPa, c_1=90 kPa, γ_0=20 kN/m^3 and γ_1=3 kN/m^3.

The comparison of shallow tunnel stability with different supporting pressures is shown in Fig. 5. The data show that the supporting pressure is advantageous to the tunnel stability. The safety factors with numerical

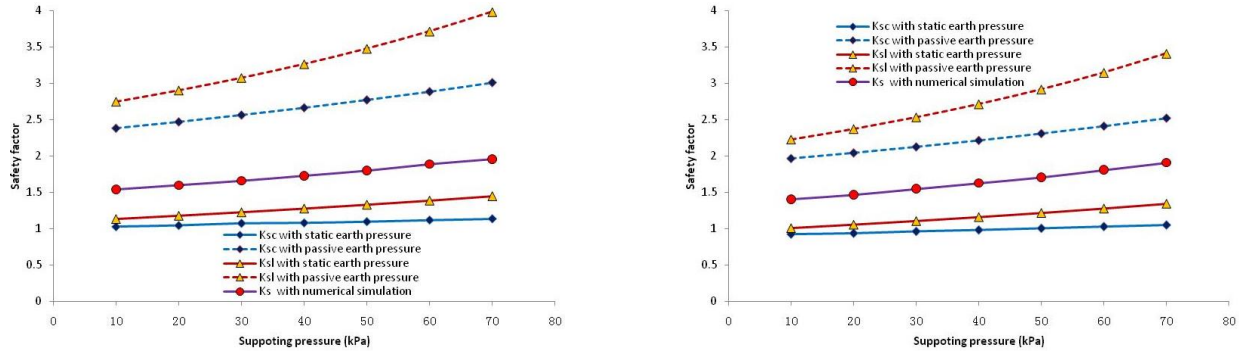

(a) In homogeneous ground (b) In inhomogeneous ground

Fig. 5 Comparison of shallow tunnel stability with different supporting pressure

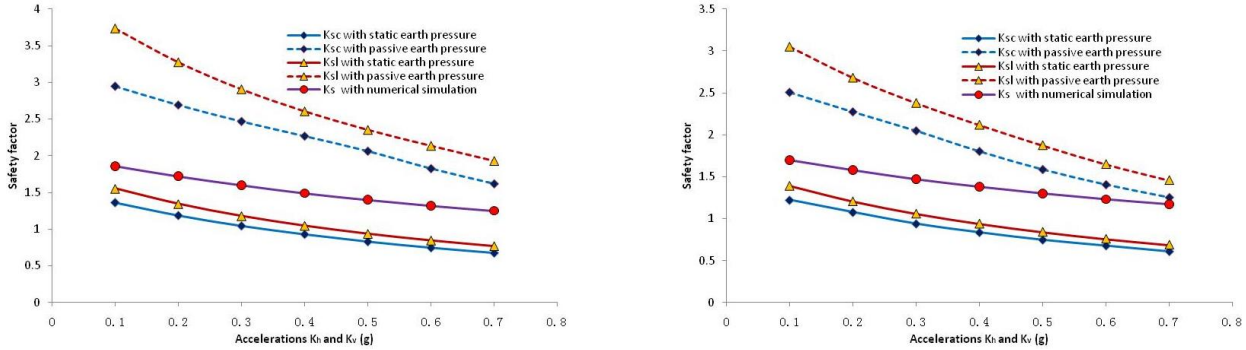

(a) In homogeneous ground (b) In inhomogeneous ground

Fig. 6 Comparison of shallow tunnel stability with different accelerations

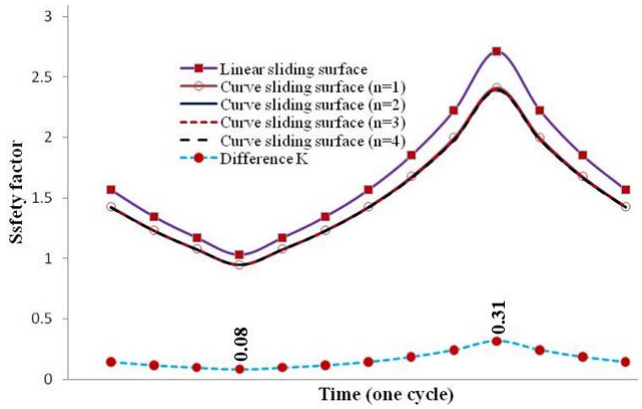

Fig. 7 Comparison of the safety factor in one earthquake cycle

simulation are greater than the analytical results with the static earth pressure (F_h=F_0), less than the analytical results with the passive earth pressure (F_h=F_p). The analytical safety factors with linear sliding surfaces are greater than with curve sliding surface.

The comparison of shallow tunnel stability with different accelerations is shown in Fig. 6. The results show the increase of acceleration leads to the decrease of the tunnel safety factor. The safety factor with linear sliding surface is greater than with curve sliding surface. When the accelerations equal 0.1g, the numerical safety factor is close to K_{sc} with static earth pressure. With the acceleration increasing, the numerical safety factor has the trend moving to K_{sc} with passive earth pressure. However, the entire numerical safety factors are greater than the analytical results with static earth pressure, less than the analytical results with passive earth pressure.

Both vertical and horizontal forces bring about the increase of shallow tunnel's stability. The tunnel excavation leads to the stress concentration around the tunnel, but it is still difficult to accurately calculate their value under different conditions. Therefore, it is conservative and reasonable to leave out F_v and define F_h equal to the integral of static earth pressure at section AB. The following analyses are completed accordingly.

4.2 Comparison of sliding surface

The distribution of the sliding surface for a shallow

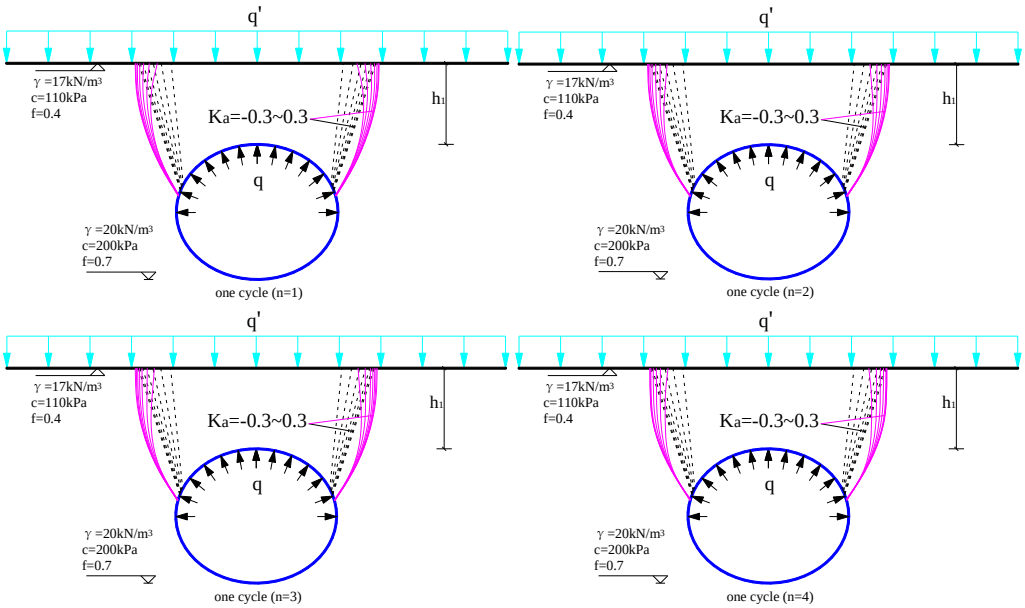

Fig. 8 Comparison of the sliding surfaces in one earthquake cycle with n=1~4

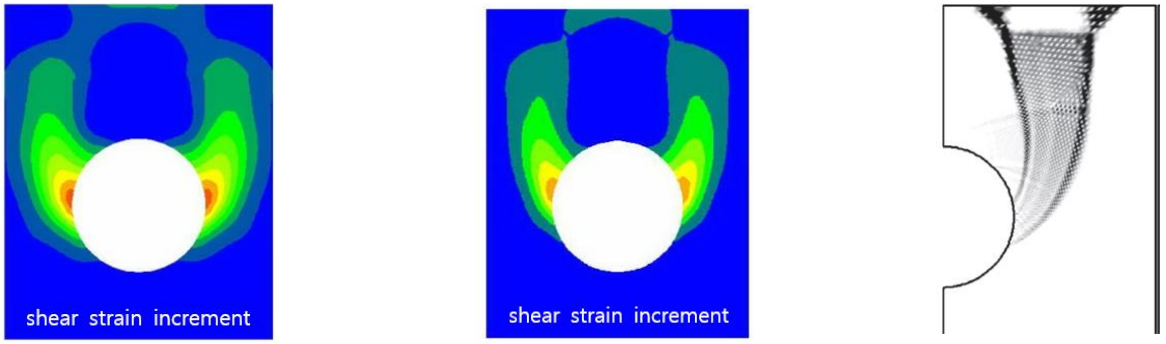

(a) Homogeneous ground (b) Inhomogeneous ground (c) Plastic multiplier field (Yamamoto *et al.* 2011)

Fig. 9 Shallow tunnel collapse mechanisms

tunnel is uncertain. Hence, it is important to determine a reasonable sliding surface to evaluate shallow tunnel stability credibly. Eqs. (1) and (2) show that the horizontal acceleration coefficient k_h belongs to ($-k_{h0}$~k_{h0}), and the vertical acceleration coefficient k_v belongs to ($-k_{v0}$~k_{v0}) in one cycle of the earthquake. To analyze the collapse mechanism of the shallow tunnel, the time of one cycle is divided into 12 parts and the acceleration interval for each part is the same value. To show the difference from each other, the curve sliding surfaces with n=1~4 and linear sliding surfaces are applied to analyze the shallow tunnel stability.

A shallow tunnel is built in the ground where a=6 m, b=5 m, h_1=6 m, q'=40 kPa, q=20 kPa, f_a=1.3, k_h=k_v=0.3, v=0.3, f_0=0.7, f_1=0.3, c_0=200 kPa, c_1=90 kPa, γ_0=20 kN/m^3 and γ_1=3 kN/m^3. The comparison of the safety factor in one earthquake cycle is shown in Fig. 7. The trends of safety factor with different sliding surfaces are similar to each other and the safety factors change greatly with the time. When the horizontal and vertical accelerations vary from -0.3 to 0.3 the safety factor with n=1 change from 0.95 to 2.41 and the largest difference of safety factor between with n=1 and with n=2 is only 0.015. Therefore, the four group safety factors on the curve sliding surface with n=1~4 are close to each other. The safety factor with linear sliding surface is greater than with curve sliding surface. The difference K represents the safety factor difference between linear sliding surface and curve sliding surface with n=2. The largest difference 0.31 appears at the largest safety factor and the smallest difference 0.08 appears at the smallest safety factor.

The comparison of the sliding surfaces in one cycle is shown in Fig. 8. The difference between curve and linear sliding surfaces are clear and the collapse region surrounded by the linear sliding surface is smaller than the region surrounded by the curve sliding surfaces. All the sliding surfaces change obviously in one earthquake cycle and the variation of linear sliding surface is wider than the curve sliding surface. The four group curve sliding surfaces with n=1~4 are similar to each other and the most part of curve sliding surfaces is increasing functions.

The safety factor is often defined as the ratio of the material strength to its shear stress on a sliding surface. In an earthquake cycle, all of the sliding surfaces comprise

Table 3 Influences on the location of point C

Tunnel depth (m)			In homogeneous ground					In inhomogeneous ground				
			2	4	6	8	10	2	4	6	8	10
Ksc with point C beyond hance	a/b	0.8	1.040	0.905	0.799	0.738	0.692	1.434	1.275	1.175	1.101	1.044
		1.0	0.936	0.801	0.727	0.672	0.633	1.255	1.134	1.057	1.000	0.955
		1.2	0.831	0.720	0.656	0.612	0.579	1.099	1.007	0.948	0.906	0.873
Ksc with point C below hance	a/b	0.8	1.034	0.880	0.787	0.722	0.673	1.457	1.280	1.174	1.099	1.041
		1.0	0.940	0.800	0.721	0.666	0.625	1.321	1.157	1.064	1.001	0.954
		1.2	0.852	0.723	0.653	0.610	0.574	1.200	1.048	0.965	0.911	0.872

Table 4 Parameters for five models

Model number	f_1/H (a_1)	c_1/H (b_1)	γ_1/H (c_1)
Model 1	0%	0%	0%
Model 2	25%	25%	25%
Model 3	50%	50%	50%
Model 4	75%	75%	75%
Model 5	100%	100%	100%

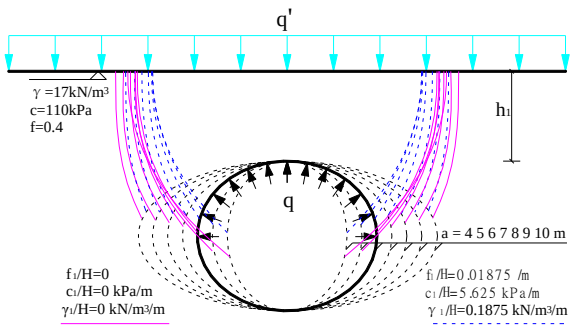

(a) Distribution of sliding surfaces

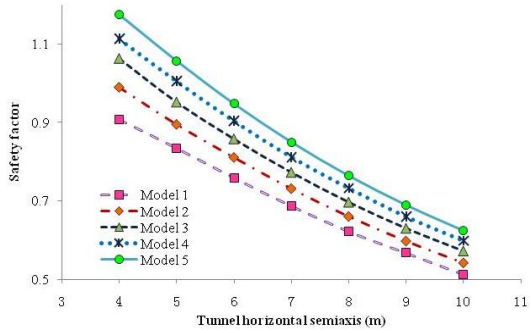

(b) Safety factor

Fig. 10 Influence of the horizontal semiaxis on shallow tunnel collapse

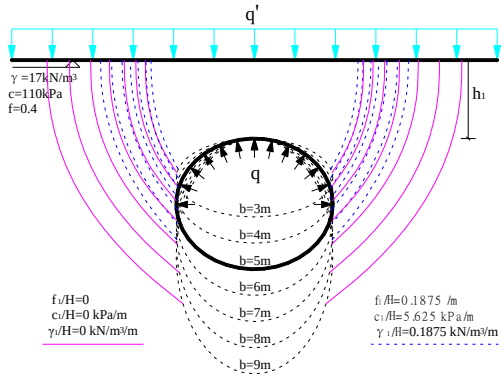

(a) Distribution of sliding surfaces

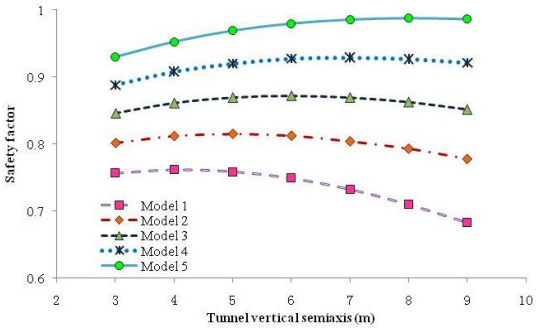

(b) Safety factor

Fig. 11 Influence of the vertical semiaxis on shallow tunnel collapse

small sliding region and the safety factors of the shallow tunnel change widely. The minimum is 0.95 and the maximum is 2.40 for safety factors with n=2. The strength is a constant in a field. This finding demonstrates that the shear stress in the small district is variable and it changes greatly. Therefore, the cyclic loading characteristics should be taken into account to evaluate tunnel stability. The shear strain increment of the shallow tunnel in homogeneous and inhomogeneous ground is shown in Fig. 9(a) and 9(b). It shows that the potential yield fields in homogeneous ground are larger than in inhomogeneous ground. Both potential yield fields are similar with each other and have excellent agreement with previous studies (Lei *et al.* 2015, Sterpi *et al.* 2004, Yamamoto *et al.* 2011), such as the plastic

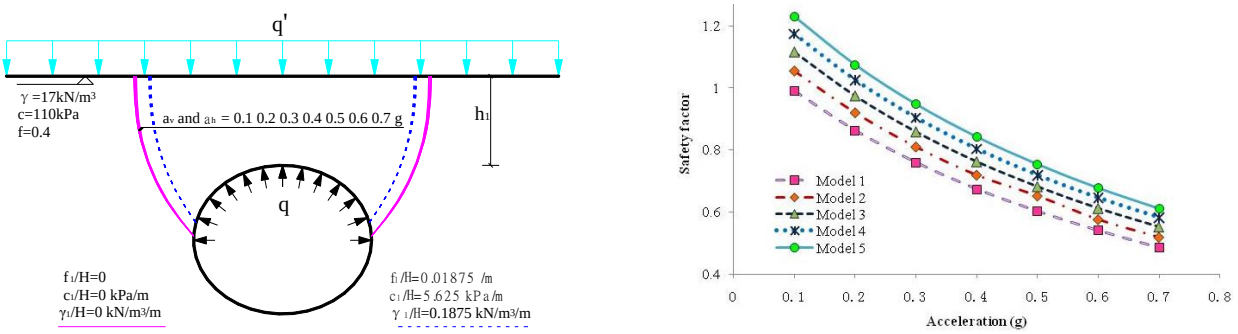

(a) Distribution of sliding surfaces (b) Safety factor

Fig. 12 Influence of the acceleration on shallow tunnel collapse

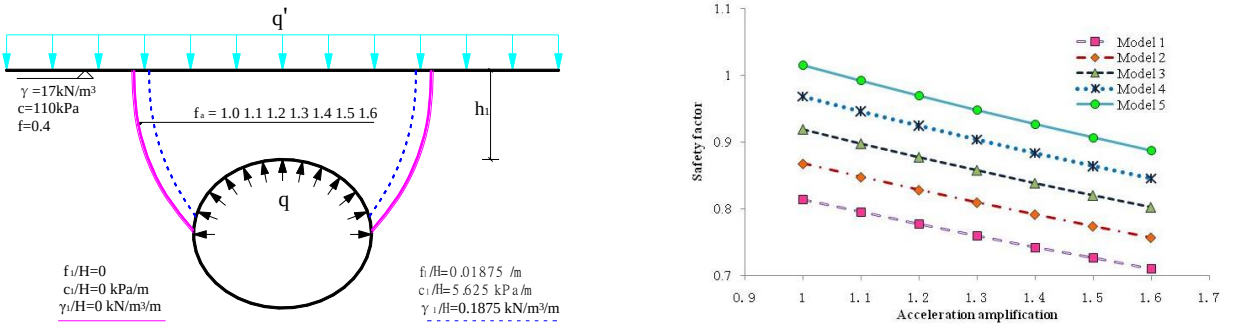

(a) Distribution of sliding surfaces (b) Safety factor

Fig. 13 Influence of the amplification factor on shallow tunnel collapse

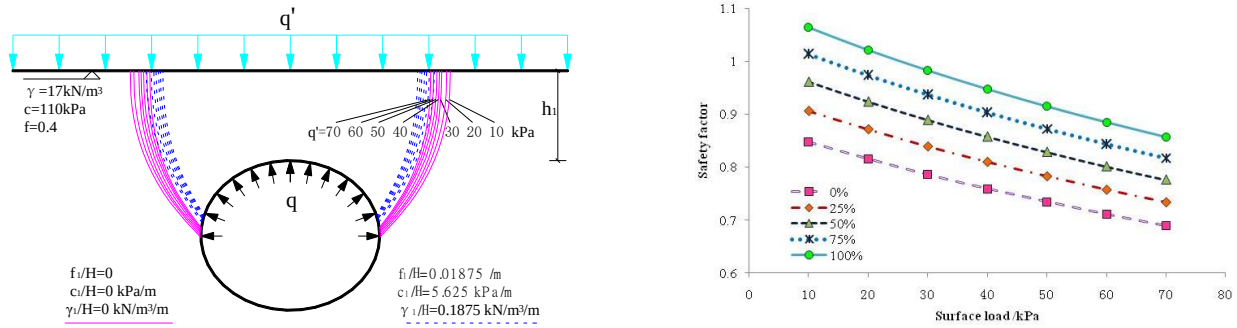

(a) Distribution of sliding surfaces (b) Safety factor

Fig. 14 Influence of the surface load on shallow tunnel collapse

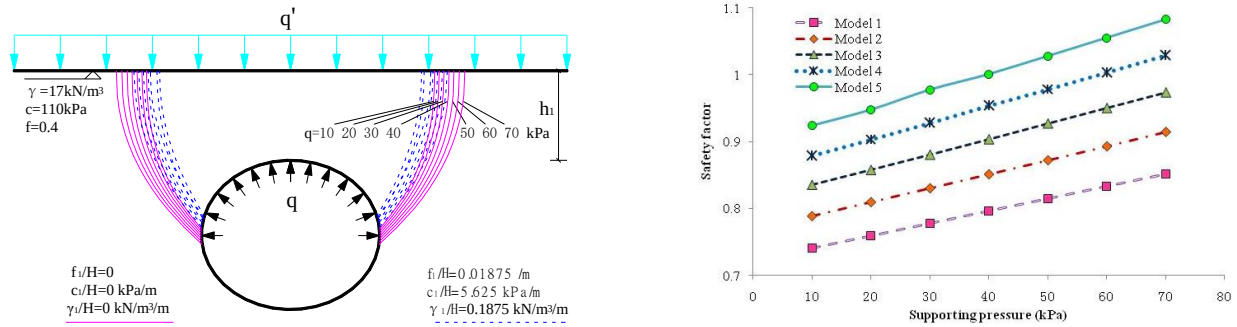

(a) Distribution of sliding surfaces (b) Safety factor

Fig. 15 Influence of the supporting pressure on shallow tunnel collapse

multiplier field in Fig. 9(c). These results show that the start damage point C is close to hance, possibly below it.

When Eq. (14) is changed into $y_0 = b - \sqrt{b^2 - (b/a\,x_0)^2}$, and then the analytical results represent point C below hance. The curved sliding surface (n=2) is applied to analyze the stability of the shallow tunnel. The sliding

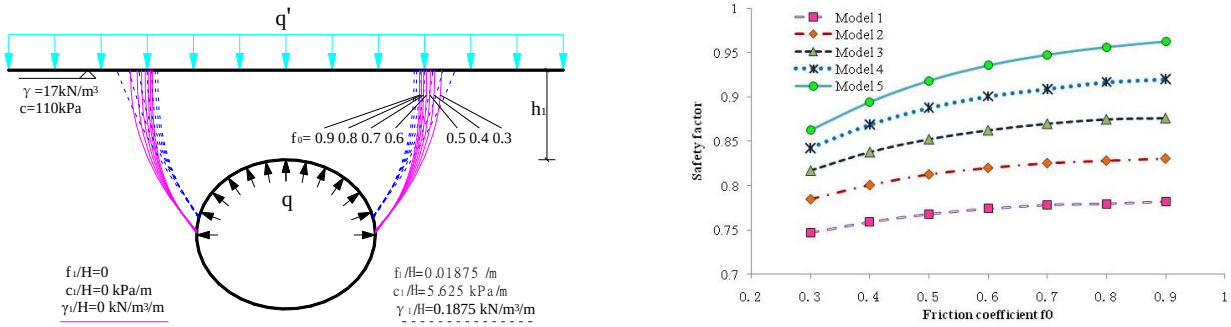

(a) Distribution of sliding surfaces (b) Safety factor

Fig. 16 Influence of friction coefficient on shallow tunnel collapse

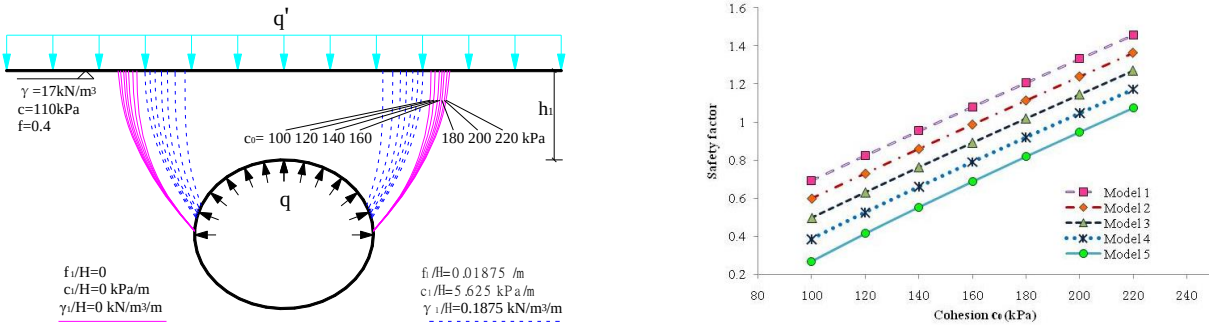

(a) Distribution of sliding surfaces (b) Safety factor

Fig. 17 Influence of the cohesion on shallow tunnel collapse

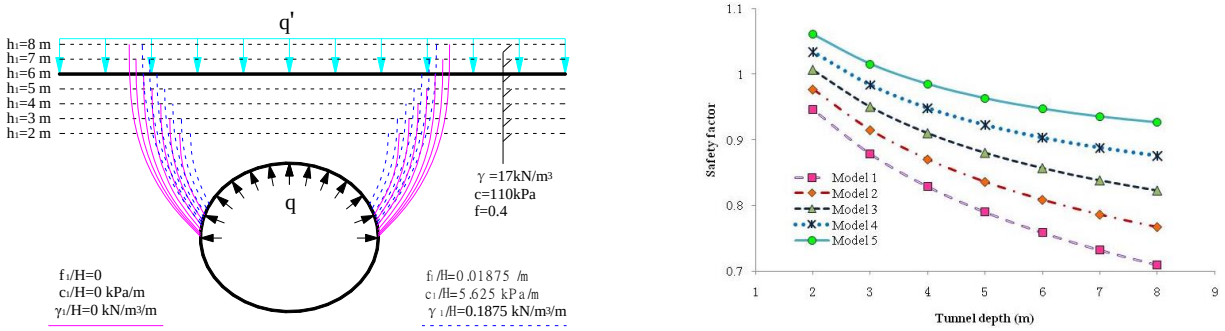

(a) Distribution of sliding surfaces (b) Safety factor

Fig. 18 Influence of the tunnel depth on shallow tunnel collapse

surface should appear where the safety factor is the minimum. The influences on the location of point C are shown in Table 3. When a/b=0.8 all the safety factors with point C beyond hance are larger than below hance in homogeneous ground. However, when the tunnel depth is less than 4 m the safety factors with point C beyond hance are smaller than below hance in homogeneous ground. When a/b increases to 1.2 point C appears beyond hance with 2-4 m tunnel depth in homogeneous ground and with 2-8 m tunnel depth in inhomogeneous ground. It shows that point C beyond and below hance should be considered. Hence, it is a reasonable choice to analyze shallow tunnel collapse mechanisms taking the both locations of point C into account and selecting the curve sliding surface(n=2) to save time and insure accuracy. And the following do accordingly.

4.3 Parameter analysis

There are many parameters influence tunnel stability and sliding surface. Engineers are interested in how they affect shallow tunnel collapse and how shallow tunnel stability can be enhanced. The ground's inhomogeneous characteristics are taken into account to analyze the shallow tunnel stability. The shallow tunnels are built in the ground where a=6 m, b=5 m, h_1=6 m, q'=40 kPa, q=20 kPa, f_a=1.3, k_h=k_v=0.3, ν=0.3, f_0=0.7, c_0=200 kPa, γ_0=20 kPa. The values of f_1/H, c_1/H and γ_1/H represent the variation along the depth. There are 5 models with different parameters, as shown in Table 4, where a_1=0.01676 m^{-1}, b_1=5.625 kPa.m^{-1} and c_1=0.01875 kN/m^3.m^{-1}. The ground is homogeneous when f_1, c_1 and γ_1 equal zero.

The influence of the horizontal semiaxis on shallow tunnel collapse is shown in Fig. 10. When the horizontal semiaxis increases from 4 m to 10 m the collapse area keeps expanding. x_0 and x_1 increase from 3.996 m and 9.016 m to

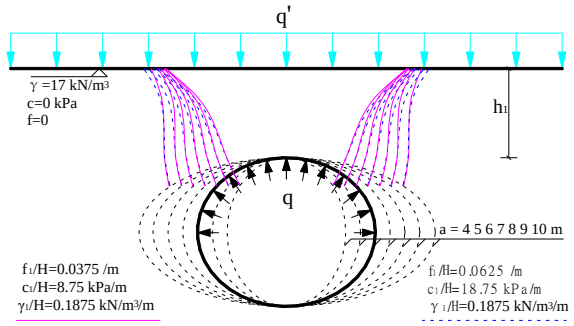

(a) Sliding surfaces with different horizontal semiaxis

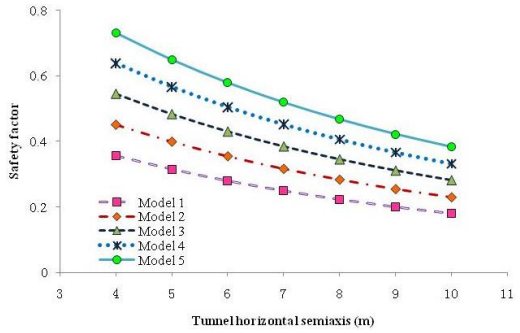

(b) Safety factor with different horizontal semiaxis

Fig. 19 Relationship between shallow tunnel collapse and horizontal semiaxis with $f_0=f_1$ and $c_0=c_1$

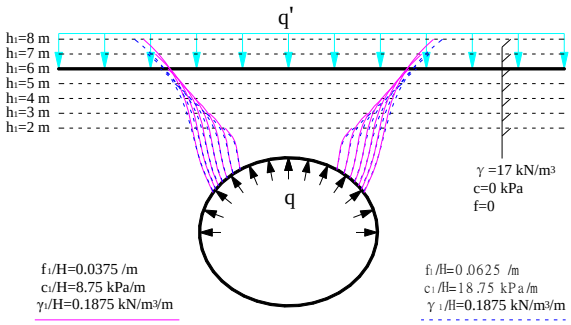

(a) Sliding surfaces at different depth

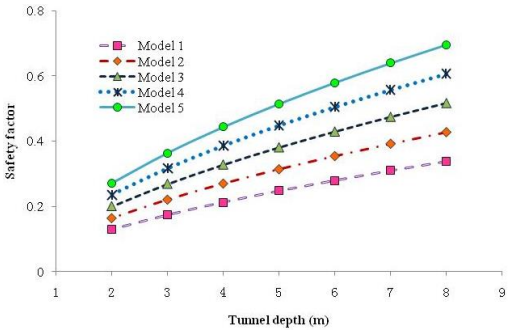

(b) Safety factor at different depth

Fig. 20 Relationship between shallow tunnel collapse and tunnel depth with $f_0=f_1$ and $c_0=c_1$

9.443 m and 10.812 m in model 5, respectively. However, the safety factor decreases from 1.174 to 0.625. When f_1/H, c_1/H and γ_1/H increase, the collapse area decreases slightly and the safety factor increases. It is clear that the horizontal semiaxis affects the shallow tunnel stability and sliding surface greatly.

The influence of the vertical semiaxis on shallow tunnel collapse is shown in Fig. 11. The vertical semiaxis has great influence on the shallow tunnel sliding surface. With b increasing from 3 m to 9 m, x_0 and x_1 increase from 5.852 m and 7.933 m to 5.941 m and 11.809 m, respectively. The collapse area enlarges greatly with an increasing b. The vertical semiaxis influence on shallow tunnel stability is uncertain. The tunnel stability decreases in model 1 when the vertical semiaxis increases, but its stability increases slightly in model 5. Therefore, the vertical semiaxis has significant influence on the sliding surface, but slight influence on tunnel stability.

The influence of the acceleration on shallow tunnel collapse is shown in Fig. 12. The acceleration has great influence on tunnel stability and very slight influence on the sliding surface. With the acceleration increasing from 0.1 g to 0.7 g the sliding surface remains almost motionless and the tunnel safety factor changes greatly, decreasing from 1.230 to 0.611 in model 5.

The influence of the amplification factor on shallow tunnel collapse is shown in Fig. 13. The increase of the amplification factor affects the sliding surface slightly. However, it leads the safety factor decrease. The safety factor reduce by 0.10-0.13 in all models when the acceleration amplification increases from 1 to 1.5.

The influence of the surface load on shallow tunnel collapse is shown in Fig. 14. The surface load increases from 10 kPa to 70 kPa, the tunnel safety factor, x_0 and x_1 in model 5 decrease from 1.065, 5.912 m and 9.670 m to 0.857, 5.782 m and 8.548 m, respectively. The surface load is detrimental to tunnel stability. The potential collapse fields in homogeneous ground are larger than in inhomogeneous ground.

The influence of the supporting pressure on shallow tunnel collapse is shown in Fig. 15. When the supporting pressure increases from 10 kPa to 70 kPa, the safety factor increases from 0.924 to 1.082, x_0 and x_1 change from 5.805 m and 8.815 m to 5.970 m and 10.552 m in model 5. It is clear that the supporting pressure is advantageous to tunnel stability, influencing the sliding surface obviously.

The influence of the friction coefficient on shallow tunnel collapse is shown in Fig. 16. The safety factor increases with the increase of the friction coefficient. x_1 decreases from 11.351 m to 8.600 m when f_0 increases from 0.3 to 0.7 in model 5. However, x_0 remains motionless. The inhomogeneous ground causes x_0 move to the vault and x_1 to vary more widely. The friction coefficient has obvious influence on tunnel sliding surface and safety factor.

The influence of cohesion on shallow tunnel collapse is shown in Fig. 17. The cohesion influence on the tunnel sliding surface and safety factor is significant. When c_0 increases from 100 kPa to 220 kPa tunnel safety factor increases from 0.267 to 1.074, x_0 and x_1 change from 5.543 m and 6.635 m to 5.865 m and 9.326 m in model 5. However, x_0 and x_1 change slightly with the variation of the cohesion in model 1.

The influence of tunnel depth on shallow tunnel collapse is shown in Fig. 18. When the tunnel depth of model 5

decreases from 8 m to 2 m the safety factor increases from 0.926 to 1.061, x_0 and x_1 decrease from 5.918 m and 9.920 m to 5.390 m and 6.681 m, respectively. The smaller the shallow tunnel depth, the greater the safety factor. The increase of tunnel depth enlarges the collapse region.

The results show that ground homogeneity has an obvious influence on tunnel stability and sliding surface. The collapse area in the homogeneous ground is larger than in the inhomogeneous ground. The horizontal semiaxis, friction coefficient, cohesion and tunnel depth are the most obvious influences on tunnel stability and the sliding surface. Therefore, the horizontal semiaxis and tunnel depth are discussed in the following with $f_0=f_1$ and $c_0=c_1$, when f_1/H and c_1/H increase from 0.0375 m^{-1} and 8.75 $kPa.m^{-1}$ to 0.0625 m^{-1} and 18.75 $kPa.m^{-1}$ with four steps to establish 5 models. The other parameters are selected from model 5.

The relationship between shallow tunnel collapse and horizontal semiaxis with $f_0=f_1$ and $c_0=c_1$ is shown in Fig. 19. The tunnel safety factor decreases and collapse area expands when the horizontal semiaxis increases. Compared to Fig. 10, it is clear that their safety factors display similar trends with horizontal semiaxis. However, their sliding surfaces are very different. The slope of sliding surface nearby ground surface is close to the lowest value, but the slope is close to the largest value in Fig. 10.

The relationship between shallow tunnel collapse and depth with $f_0=f_1$ and $c_0=c_1$is shown in Fig. 20. The increase of tunnel depth leads to the increase of safety factor and the expansion of the collapse area. In comparison with Fig. 18, many results change greatly. Firstly, the tunnel safety factor increases with tunnel depth because the soil strength increases very quickly with the tunnel depth. However, it decreases in Fig. 18. Secondly, the slope of sliding surface near the tunnel increases, and it subsequently decreases when close to the ground surface. Nevertheless, the slope of sliding surface continues to increase in Fig. 18.

5. Conclusions

Based on the limit equilibrium method and variational principle, a solution is presented to analyze shallow tunnel's seismic collapse mechanism in inhomogeneous ground. The finite difference method is applied to compare with it. Thus, the following conclusions become clear.

• The safety factors of numerical simulation are greater than the analytical results with $F_h=F_0$, less than the analytical results with $F_h=F_p$ when $F_v=0$. Therefore, it is conservative to define F_h equal to the integral of static earth pressure. The safety factor of shallow tunnel changes greatly in one earthquake cycle. Hence, the cyclic loading characteristics should be taken into account to evaluate tunnel seismic stability.

• The curve sliding surface shows good agreement with the numerical results and the previous studies. It is a good choice to analyze shallow tunnel collapse mechanism with the curve sliding surface (n=2).

• The parameter analyses show that the four most significant influences on tunnel safety factor are the horizontal semiaxis, acceleration, ground cohesion and homogeneity. In addition, the four most significant influences on tunnel sliding surface are the horizontal semiaxis, vertical semiaxis, tunnel depth and ground homogeneity. Strengthening cohesion, reducing the horizontal semiaxis and setting the tunnel into good ground are applicable approaches to enhance shallow tunnel stability.

Acknowledgments

The research described in this paper was financially supported by the National Science Foundation of China (50334060 and 41672304) and the Sichuan Province Education Department's Scientific Research Foundation of China (11ZB055 and 16TD0006).

References

Amorosi, A. and Boldini, D. (2009), "Numerical modelling of the transverse dynamic behaviour of circular tunnels in clayey soils", *Soil Dyn. Earthq. Eng.*, **29**(6), 1059-1072. https://doi.org/ 10.1016/j.soildyn.2008.12.004.

Argyroudis, S.A. and Pitilakis, K.D. (2012), "Seismic fragility curves of shallow tunnels in alluvial deposits", *Soil Dyn. Earthq. Eng.*, **35**, 1-12. https://doi.org/ 10.1016/j.soildyn.2011.11.004.

Atkinson, J. and Potts, D. (1977), "Stability of a shallow circular tunnel in cohesionless soil", *Geotechnique*, **27**(2), 203-215. https://doi.org/ 10.1680/geot.1977.27.2.203.

Azadi, M. and Hosseini, S.M.M. (2010), "Analyses of the effect of seismic behavior of shallow tunnels in liquefiable grounds", *Tunn. Undergr. Sp. Tech.*, **25**(5), 543-552. https://doi.org/10.1016/j.tust.2010.03.003.

Bilotta, E., Lanzano, G., Russo, G., Santucci de Magistris, F., Aiello, V., Conte, E., Silvestri, F. and Valentino, M. (2007), "Pseudostatic and dynamic analyses of tunnels in transversal and longitudinal directions", *Proceedings of the 4th International Conference on Earthquake Geotechnical Engineering*, Thessaloniki, Greece.

Davis, E., Gunn, M., Mair, R. and Seneviratine, H. (1980), "The stability of shallow tunnels and underground openings in cohesive material", *Geotechnique*, **30**(4), 397-416. https://doi.org/10.1680/geot.1980.30.4.397.

Fraldi, M. and Guarracino, F. (2009), "Limit analysis of collapse mechanisms in cavities and tunnels according to the Hoek-Brown failure criterion", *Int. J. Rock Mech. Min. Sci.*, **46**(4), 665-673. https://doi.org/ 10.1016/j.ijrmms.2008.09.014.

Fraldi, M. and Guarracino, F. (2012), "Limit analysis of progressive tunnel failure of tunnels in Hoek-Brown rock masses", *Int. J. Rock Mech. Min. Sci.*, **50**, 170-173. https://doi.org/ 10.1016/j.ijrmms.2011.12.009.

Ghosh, S. (2010), "Pseudo-dynamic active force and pressure behind battered retaining wall supporting inclined backfill", *Soil Dyn. Earthq. Eng.*, **30**(11), 1226-1232. https://doi.org/ 10.1016/j.soildyn.2010.05.003.

Gomes, R.C., Gouveia, F., Torcato, D. and Santos, J. (2015), "Seismic response of shallow circular tunnels in two-layered ground", *Soil Dyn. Earthq. Eng.*, **75**, 37-43. https://doi.org/ 10.1016/j.soildyn.2015.03.012.

Huang, F. and Yang, X. (2011), "Upper bound limit analysis of collapse shape for circular tunnel subjected to pore pressure based on the Hoek-Brown failure criterion", *Tunn. Undergr. Sp. Tech.*, **26**(5), 614-618. https://doi.org/ 10.1016/j.tust.2011.04.002.

Huang, F., Zhang, D.B., Sun, Z.B. and Jin, Q.Y. (2012), "Upper bound solutions of stability factor of shallow tunnels in saturated soil based on strength reduction technique", *J. Central South Univ.*, **19**, 2008-2015. https://doi.org/ 10.1007/s11771-012-1238-4.

Jaky, J. (1944), "The coefficient of earth pressure at rest", *J. Soc. Hungarian Arch. Eng.*, **78**(22), 355-358. https://doi.org/ 10.1139/t93-056

Jones, S. and Hunt, H. (2012), "Predicting surface vibration from underground railways through inhomogeneous soil", *J. Sound Vib.*, **331**(9), 2055-2069. https://doi.org/ 10.1016/j.jsv.2011.12.032.

Kolathayar, S. and Ghosh, P. (2009), "Seismic active earth pressure on walls with bilinear backface using pseudo-dynamic approach", *Comput. Geotech.*, **36**(7), 1229-1236. https://doi.org/ 10.1016/j.compgeo.2009.05.015.

Lei, M., Peng, L. and Shi, C. (2014), "Calculation of the surrounding rock pressure on a shallow buried tunnel using linear and nonlinear failure criteria", *Automat. Constr.*, **37**, 191-195. https://doi.org/ 10.1016/j.autcon.2013.08.001.

Lei, M., Peng, L. and Shi, C. (2015), "Model test to investigate the failure mechanisms and lining stress characteristics of shallow buried tunnels under unsymmetrical loading", *Tunn. Undergr. Sp. Tech.*, **46**, 64-75. https://doi.org/10.1016/j.tust.2014.11.003.

Munwar Basha, B. and Sivakumar Babu, G.L. (2010), "Reliability assessment of internal stability of reinforced soil structures: A pseudo-dynamic approach", *Soil Dyn. Earthq. Eng.*, **30**(5), 336-353. https://doi.org/ 10.1016/j.soildyn.2009.12.007.

Phoon, K.K. and Kulhawy, F.H. (1999), "Characterization of geotechnical variability", *Can. Geotech. J.*, **36**(4), 612-624. https://doi.org/ 10.1139/cgj-36-4-612

Pitilakis, K., Tsinidis, G., Leanza, A. and Maugeri, M. (2014), "Seismic behaviour of circular tunnels accounting for above ground structures interaction effects", *Soil Dyn. Earthq. Eng.*, **67**, 1-15. https://doi.org/ 10.1016/j.soildyn.2014.08.009.

Popescu, R., Deodatis, G. and Nobahar, A. (2005), "Effects of random heterogeneity of soil properties on bearing capacity", *Probab. Eng. Mech.*, **20**(4), 324-341. https://doi.org/10.1016/j.probengmech.2005.06.003.

Saada, Z., Maghous, S. and Garnier, D. (2013), "Pseudo-static analysis of tunnel face stability using the generalized Hoek-Brown strength criterion", *Int. J. Numer. Anal. Meth. Geomech.*, **37**(18), 3194-3212. https://doi.org/ 10.1002/nag.2185.

Sahoo, J.P. and Kumar, J. (2013), "Stability of long unsupported twin circular tunnels in soils", *Tunn. Undergr. Sp. Tech.*, **38**, 326-335. https://doi.org/10.1016/j.tust.2013.07.005.

Sahoo, J.P. and Kumar, J. (2014), "Stability of a circular tunnel in presence of pseudostatic seismic body forces", *Tunn. Undergr. Sp. Tech.*, **42**, 264-276. https://doi.org/ 10.1016/j.tust.2014.03.003.

Shen, Y., Gao, B., Yang, X. and Tao, S. (2014), "Seismic damage mechanism and dynamic deformation characteristic analysis of mountain tunnel after Wenchuan earthquake", *Eng. Geol.*, **180**, 85-98. https://doi.org/10.1016/j.enggeo.2014.07.017.

Sterpi, D. and Cividini, A. (2004), "A physical and numerical investigation on the stability of shallow tunnels in strain softening media", *Rock Mech. Rock Eng.*, **37**(4), 277-298. https://doi.org/10.1007/s00603-003-0021-0.

Tao, L., Hou, S., Zhao, X., Qiu, W., Li, T., Liu, C. and Wang, K. (2015),"3-D shell analysis of structure in portal section of mountain tunnel under seismic SH wave action", *Tunn. Undergr. Sp. Tech.*, **46**, 116-124. https://doi.org/10.1016/j.tust.2014.11.001.

Wang, T., Zhou, G., Wang, J. and Zhao, X. (2016), "Stochastic analysis for the uncertain temperature field of tunnel in cold regions", *Tunn. Undergr. Sp. Tech.*, **59**, 7-15. https://doi.org/10.1016/j.tust.2016.06.009.

Wang, W., Wang, T., Su, J., Lin, C., Seng, C. and Huang. T. (2001), "Assessment of damage in mountain tunnels due to the Taiwan Chi-Chi Earthquake", *Tunn. Undergr. Sp. Tech.*, **16**(3), 133-150. https://doi.org/10.1016/S0886-7798(01)00047-5.

Wang, Z. and Zhang, Z. (2013), "Seismic damage classification and risk assessment of mountain tunnels with a validation for the 2008 Wenchuan earthquake", *Soil Dyn. Earthq. Eng.*, **45**, 45-55. https://doi.org/10.1016/j.soildyn.2012.11.002.

Yamamoto, K., Lyamin, A.V., Wilson, D.W., Sloan, S.W. and Abbo, A.J. (2011), "Stability of a circular tunnel in cohesive-frictional soil subjected to surcharge loading", *Comput. Geotech.*, **38**(4), 504-514. https://doi.org/10.1016/j.compgeo.2011.02.014.

Yang, X. and Huang, F. (2011), "Collapse mechanism of shallow tunnel based on nonlinear Hoek-Brown failure criterion", *Tunn. Undergr. Sp. Tech.*, **26**(6), 686-691. https://doi.org/10.1016/j.tust.2011.05.008.

Yang, X.L. and Long, Z.X. (2015), "Roof collapse of shallow tunnels with limit analysis method", *J. Central South Univ.*, **22**, 1929-1936. https://doi.org/ 10.1007/s11771-015-2712-6.

GC